ISOCAM mapping of the Whirlpool galaxy M 51[*]

M. Sauvage[1], **J. Blommaert**[2], **F. Boulanger**[3], **C.J. Cesarsky**[3], **D.A. Cesarsky**[1], **F.X. Désert**[3], **D. Elbaz**[1], **P. Gallais**[1,2], **G. Joncas**[4], **L. Metcalfe**[2], **K. Okumura**[2], **S. Ott**[2], **R. Siebenmorgen**[2], **J.L. Starck**[1], **D. Tran**[1], and **L. Vigroux**[1]

[1] CEA/DSM/DAPNIA/Service d'Astrophysique, C.E. Saclay, F-91191 Gif-sur-Yvette Cedex, France
[2] ISO Science Operations Centre, Astrophysics Division of ESA, Villafranca del Castillo, P.O. Box 50727, E-28080 Madrid, Spain
[3] Institut d'Astrophysique Spatiale, Université Paris-Sud, Bât. 121, F-91405, Orsay France
[4] Département de Physique, Obs. Astronomique du Mont Mégantic, Université Laval Sainte-Foy, Québec G1K7PK, Canada

Received 16 July 1996 / Accepted 29 August 1996

Abstract. We have obtained the first images of the 6.75 and $15\mu m$ continuum emission in the Whirlpool galaxy with ISO-CAM, the infrared camera of the ISO[1]. These data reveal the well-developed, spiral arms of the galaxy, in addition to diffuse emission between arms and in the outer regions of the disk. There is a striking correspondence with the $15\mu m$ emission and the $H\alpha$ emission over the galaxy. We tighten this link by looking at the properties of the individual HII regions and show that the $15\mu m$ emission traces massive star formation and is not affected by extinction as is $H\alpha$. The data show systematic mid-infrared color variations perpendicular to the arms, which we interpret as two distinct dust components contributing to the mid-infrared emission. We examine the implication of these color variations in light of our current understanding of dust at these wavelength.

Key words: galaxies: individual: M 51 – galaxies: ISM – galaxies: spiral – infrared: interstellar: continuum – stars: formation

1. Introduction

M 51 (NGC 5194) and its companion NGC 5195 constitute a textbook example of an interacting pair of galaxies. M 51 is a grand-design spiral galaxy (Sbc I-II in the Shapley-Ames catalog), somewhat perturbed by its companion. The arms are very thick, and obscuring dust lanes are seen all across the face of the galaxy (see e.g. Sage, 1989). In the arms, star formation is proceeding actively, as revealed, for example, by the UV data of Hill et al. (1996).

Send offprint requests to: msauvage@cea.fr

[1] See Kessler et al. 1996.

In this *Letter* we present the initial results of a complete map of M 51 using ISOCAM (Cesarsky *et al.* 1996) at $6.75\mu m$ and $15\mu m$.

2. Observations and Data Reduction

Broad-band MIR mapping. A $13' \times 13'$ field was mapped in LW2 (5 to 8 μm) and LW3 (12 to 17 μm) using ISOCAM, the infrared camera of ISO (Kessler *et al.* 1966). A raster map of 10×10 positions was constructed, with an array of 32×32 pixels, and $3''$ pixel field of view giving a spatial resolution of $\simeq 5 - 8''$. Spacing between each successive positions of the raster was $84''$ in both directions, resulting in $12''$ overlaps.

Data were reduced with the CAM Interactive Analysis software (CIA)[2]. The basic steps, dark current subtraction and cosmic hit removal are described in Siebenmorgen et al. (1996). Transients, due to detector memory effects (see Cesarsky et al., 1996), were corrected with a double exponential method and an inversion method (Abergel et al., 1996; Stark et al., 1996).

We took advantage of the large field observed to derive the flat-field from the observations of the background regions. The rms around the background level in the final images are 4.3 $\mu Jy/''^2$ and 5.7 $\mu Jy/''^2$. Important sources of uncertainties are, in decreasing order, transient effect corrections, photometric conversion factors, and flat-field errors, giving a total estimated uncertainty of 20-30%.

$H\alpha$ mapping. As star formation plays a crucial part in determining the MIR properties of galaxies, $H\alpha$ data were obtained by one of us (G. Joncas) at the Mont Mégantic Observatory. The $H\alpha$ map was produced by scaling the star fluxes in the narrow band image to their counterparts in the broad-band image and subtracting the R image from the $H\alpha$ image. The point spread function was determined using images of stars in the field. For cross-comparison, we degraded the $H\alpha$ image to the LW3 resolution ($\simeq 8''$) and resampled it to 3" pixels.
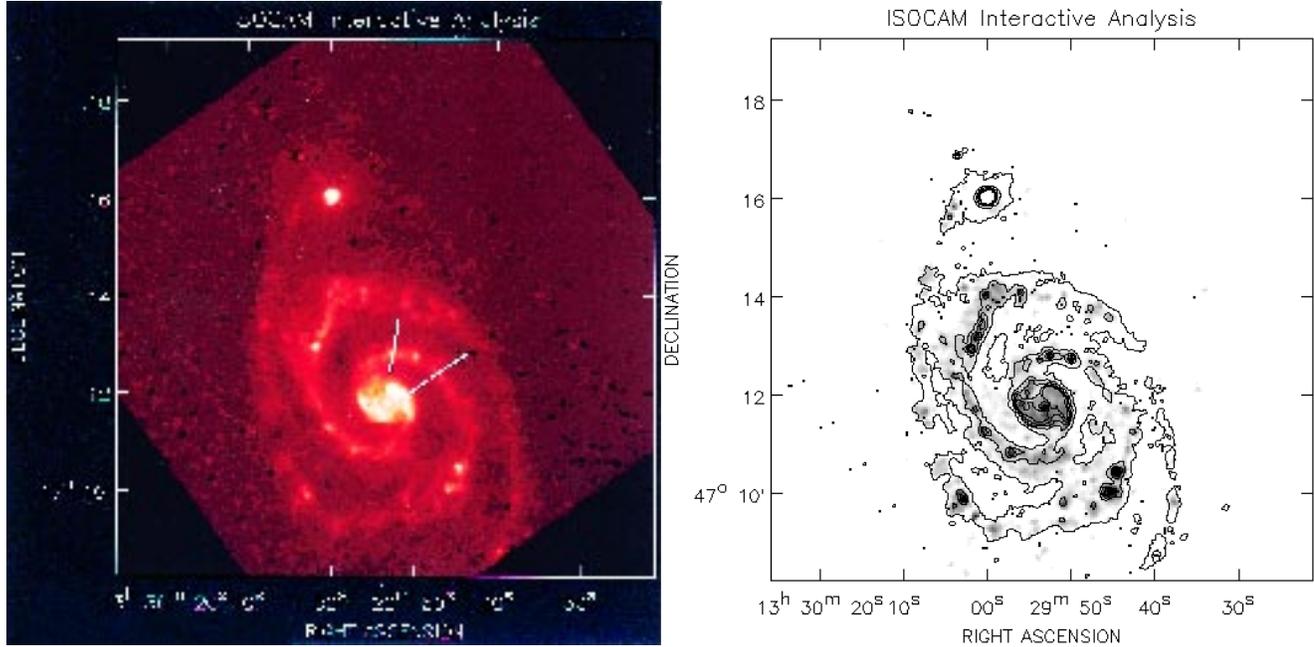
Fig. 1. (a) The LW3 (15μm) raster map of M 51. In order to reveal the low-level emission, the linear intensity scale was saturated well below the maximum level in the image (i.e. the nucleus of NGC 5195). Numerous well-know Hıı regions are detected all the way to the tip of the arm overlaping the companion galaxy in the north, NGC 5195. The source NE of NGC 5195 is a memory effect. Black lines indicate the directions along which the cuts in figure 3 are performed. (b) An Hα grey-scale image with LW3 contours superimposed. Contours of the LW3 image start at the 6σ level and are spaced by 10σ. The correspondence is so striking that the contours seems in fact to be those of Hα. The correspondence breaks down at NGC 5195.

3. MIR Morphology of the M 51 Disk

In figure 1a we present the raster map of M 51 in the LW3 (15μm) band, with a linear intensity scale. The most striking feature in this image is the spiral pattern. The arms are extremely well defined and can be followed from $\simeq 25''$ beyond the nucleus to the outskirts of the galaxy, having circled $\simeq 450°$ for the western arm, and $\simeq 540°$ for the eastern arm, all the way to the east of NGC 5195.

There is also definite diffuse emission in the interarm region, evident in the contours which begin at the 6σ level, in figure 1b. In fact, on azimuthally averaged radial profiles, emission is still detected $170''$ away from the nucleus. Thus the MIR disk is as large as the FIR disk and extends well into the Hı ring of M 51 (see Smith, 1982).

The nuclear region of M 51 also presents interesting structure: the arms seem to connect to a ring-like structure that surrounds a sharply peaked source, probably heated by the AGN in M 51.

In figure 1b we compare the Hα and LW3 images of M 51. There is almost a one-to-one correspondence: all the Hıı regions correspond to peaks in the MIR map. This clearly emphasizes the link between the two emission processes: star formation is the main provider of energy for the dust particles we detect at 15μm. The correspondence does not exist toward the companion galaxy in the north, NGC 5195, where Hα is in absorption while the MIR image show a strong point-like source (see Boulade et al., 1996).

Bersier et al. (1994) and Petit et al. (1996) compared the Hα and UV (2000Å) morphology of M 51 and observed broader UV arms as well as a systematic displacement between the two images; the UV peaks being shifted by 7-11″ downstream from the Hα peaks. They interpret this as being due to the combined effects of (1) stars required to produce UV light live longer than ionizing stars and (2) extinction is likely to be higher in the arms than in the interarm region.

Let us then use this marked difference of spatial distribution between ionizing and hot, non-ionizing star to investigate the heating sources for LW3 emission. The width of the arms in the LW3 image is $\simeq 15''$ FWHM (see figure 3), i.e. similar to the FWHM of the Hα arms. No systematic displacement is seen between the Hα and LW3 maps. Therefore it appears that LW3 is more strongly linked to the ionizing stars than to the non-ionizing UV emitting ones. This may reflect the fact that only in or near Hıı regions will grains be hot enough to contribute a continuum emission in the LW3 band (seen as an emission increasing with wavelength). In softer radiation environments, the emission detected in LW3 is rather low (see Boulade et al., 1996) or even decreasing with respect to the wavelength (see Boulanger et al., 1996). Thus, the LW3 emission does seem to trace star formation well. It is also detected outside of Hıı regions, yet at much lower levels. Whether this dust is heated by the broader UV arms or by the local stellar population remains to be analyzed.
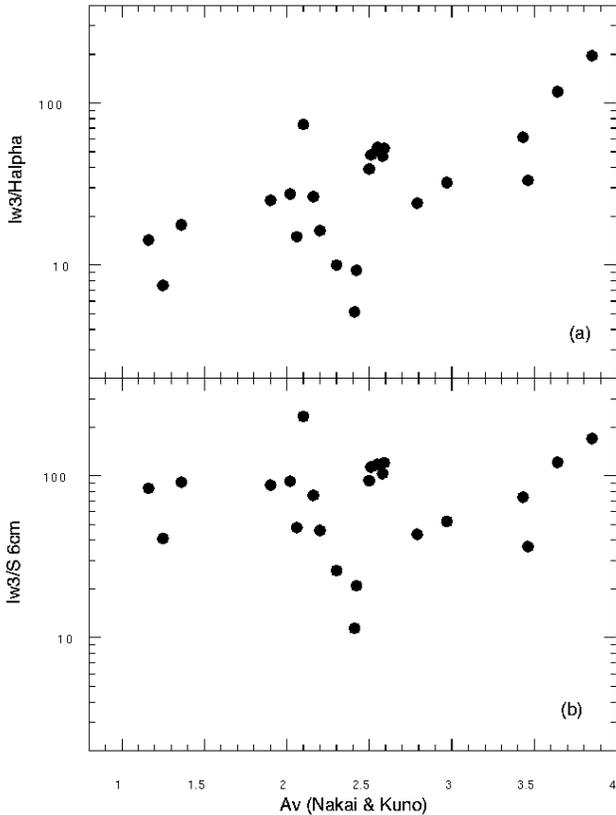
Fig. 2. (a) The LW3/Hα ratio (mJy/10^{-13} erg cm^{-2}) versus A$_V$ from Nakai & Kuno 1995. Although the scatter is large, and can be mostly attributed to uncertainties in the LW3 flux, a clear trend is seen for a correlation of the two quantities ($r = 0.79$). (b) Variation of the LW3/S$_{6cm}$(thermal) ratio with A$_V$. In this case, no correlation is seen ($r = 0.15$).

4. HII Regions in M51

In this section we combine our data on HII regions with that of van der Hulst et al. (1988) to examine the nature of the link between LW3 flux and star formation. We extracted the LW3 flux for 23 HII regions that could clearly be isolated on our map. Photometry was performed by summing the flux inside radii adjusted to each source and subtracting an estimated background. Since determining where the background is to be taken is the most difficult step in determining the flux, we used two methods: one assuming the same background for all sources, and another with the background as the median of the flux outside the integrating radius. We find that the correlations we present here are independent of the method used.

For all these HII regions we compile the Hα and thermal 6 cm radio fluxes from van der Hulst et al. (1988) and A$_V$ from Nakai & Kuno (1995). Both Hα and S$_{6cm}$ are related to the ionizing stellar population although only Hα can be effected by extinction. In figure 2 we compare the variation of the two ratios (a) LW3/Hα and (b) LW3/S$_{6cm}$ for our sample with A$_V$. Given the uncertainties involved both in the correction of transient effects and in the extraction of source photometry, most of the

scatter in both graphs is due to the determination of the LW3 flux.

Although the distribution of points shows some similarity, a correlation is present in figure 2a and not in figure 2b: the LW3/Hα ratio increases with A$_V$ while the LW3/S$_{6cm}$ ratio does not appear to depend on the extinction (the correlation coefficients are respectively 0.79 and 0.15). In fact, when the Hα emission is corrected for extinction with A$_V$, the LW3/Hα ratio becomes quite constant. An interpretation of these trends consistent with the tight spatial correlation shown in section 3 is the following: LW3 is indeed mostly reprocessing of the radiation from young ionizing stars but, not surprisingly, it is uneffected by extinction, contrary to Hα. As the derivation of the thermal radio flux is not straightforward and implies observations at different radio wavelengths, LW3 could prove an efficient way to derive star-forming properties when A$_V$ is $\gtrsim 1 - 2$ (see Vigroux et al., 1996).

5. Infrared Colors of M 51

The LW2 and LW3 filters sample two different kinds of emission: the LW3 filter (12-18μm) collects mostly continuum emission as well as, if present, [NeII] (12.8μm) and [NeIII] (15.5μm). The LW2 filter (5-8.5μm) collects almost exclusively emission from the so-called PAH bands at 6.2, 7.7 and 8.6μm. The LW2/LW3 ratio should thus reveal information on the heating sources and emission mechanisms.

To demonstrate color variations in the disk of M 51, we plot the LW2/LW3 ratio in figure 3 in two cuts perpendicular to the spiral arms of M 51 (identified on figure 1a). On these cuts it is clear that the ratio drops in the arms or in the nuclear region. More generally, the LW2/LW3 ratio decreases as the mean MIR brightness increases, i.e. in the star forming regions.

This behavior already implies that the emission sampled at LW2 and LW3 comes from two distinct components of the dust phase. Otherwise, as the interstellar radiation field decreases, one would either observe a decrease of the ratio, corresponding to cooler temperature in the case of grains in thermal equilibrium, or a constant, in the case of impulsive heating. A possible explanation for the observed behavior is the following: in LW3 we detect the short wavelength edge of a continuum provided by hot small grains with a nearly thermal behavior, heated by ionizing photons as shown in section 3 and 4. As the heating flux drops, their temperature decreases and therefore the emission falls exponentially, such as in the case of classical black-body emission. In the LW2 band we collect feature emission. If this emission comes from PAHs, then the impulsive heating mechanism implies that their emission will follow rather linearly the decrease of the heating intensity, leading to an increase of the LW2/LW3 ratio (see e.g. Désert et al., 1990). We should point out, however, that the observed color behavior can also be explained if the grains emitting in the LW2 band can be heated by non-ionizing or even optical photons (see e.g. Guillois et al., 1996). Indeed one can expect that away from the star forming regions, these dominate the radiation field.
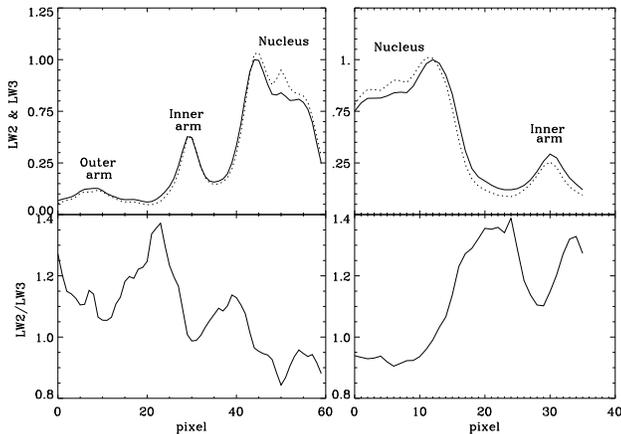
Fig. 3. The LW2/LW3 ratio along cuts perpendicular to the spiral arms at the locations indicated in figure 1a. The top panels show the brightness profiles normalized to their respective peak LW2 flux (continuous: LW2, dotted: LW3) and the bottom ones the color profile. It is quite clear that arm crossing is associated with a decrease of the ratio. Given that the cuts are taken respectively at $45°$ and $90°$ of the scan direction, these behaviors are extremely unlikely to be caused by transients effects.

Note that the color trends in M 51 are also found in Galactic H II regions (Cesarsky et al., 1996) and that the color of the interarm regions , $\simeq 1.2$-1.4, is similar to that observed in the halo parts of the ρ Oph cloud (see Abergel et al., 1996).

6. Conclusions

The ISOCAM observations of the M 51 disk in the LW2 and LW3 filter reveal a well defined, spiral galaxy. Diffuse emission is also detected in the interarm region as well as in the outer parts of the disk. Comparison with Hα data shows that current star formation plays a crucial part in the heating of the dust detected in LW3. Furthermore we show that the LW3/Hα ratio is clearly correlated to the visual extinction, implying that in star forming regions, LW3 has the potential to provide a valuable estimation of the input of ionizing stars. We also show that definite color variations occur, indicating that the LW2 and LW3 emission probably comes from two different dust components. Whether LW2 is as tightly related to recent star formation as LW3 is unclear until the bearers of this emission and their heating mechanism are definitely identified.

References

Abergel, A. et al. 1996, *this volume*
Bersier, D., Blecha, A., Golay, M., Martinet, L. 1994, A&A, 37, 45
Boulade, O. et al., 1996, *this volume*
Boulanger, F., et al. 1996, *this volume*
Cesarsky, C. et al., 1996, *this volume*
Cesarsky, D. et al., 1996, *this volume*
Désert, F.X., Boulanger, F., Puget, J.L., 1990, A&A, 237, 215
Hill, J.K., Waller, W.H., Cornett, R.H., et al., 1996, ApJ, *preprint*

van der Hulst, J.M., Kennicutt, R.C., Crane, P.C., Rots, A.H. 1988, A&A, 195, 38
Kessler, M.F., et al. 1996, A&A, *this volume*
Nakai, N., Kuno, N.1995, PASJ, 47, 761
Guillois, O., Nenner, I., Papoular, R., Reynaud, C. 1996, ApJ, 464, 810
Petit, H., Hua, C.T., Bersier, D., Courtès, G. 1996, A&A, 309, 446
Sage, L.J. 1989, ApJ, 344, 200
Siebenmorgen, R., Starck, J.L., Cesarsky, D.A., Guest, S., Sauvage, M. 1996, "ISOCAM Data Users Manual", ESA, SAI/95-222/Dc
Smith, J. 1982, ApJ, 261, 463
Stark, J.-L., Claret, A. and Siebenmorgan, R., C.E.A. Technical Report, March 1996
Vigroux, L. et al., 1996, *this volume*